

Influence of conventional and cryogenic piezo peening on bending fatigue strength of hardened bearing steel AISI 52100

Alexander Klumpp^{a,*}, Mehmet Ali Tamam^a, Florian Vollert^a, Stefan Dietrich^a, Volker Schulze^a
^a* Karlsruhe Institute of Technology, Germany, alexander.klumpp@kit.edu

Keywords: Piezo Peening (“PP”), Retained Austenite (“RA”), Residual Stress (“RS”), Machine Hammer Peening (“MHP”), Fatigue Strength, Modified Treatment, Cryogenic (“cryo”)

Introduction

Machine hammer peening (MHP) treatments have become a crucial process step in the fabrication of molds and dies, which is mainly due to the generation of smooth surfaces in connection with compressive residual stresses (RS) and work-hardening [1]. Developed at Karlsruhe Institute of Technology (KIT), piezo peening (PP) is a modern MHP treatment capable of generating a large bandwidth of (anisotropic) RS and work-hardening states with penetration depths between 100 μm and 1 mm [2, 3]. By this means, greatly enhanced fatigue behavior could be achieved on quenched and tempered low alloy steel AISI 4140 in previous studies [4].

Fig. 1 shows a schematic representation of the utilized PP device [2]. The spherical hammer head is brought into oscillation by the piezo actuator with specific frequency and stroke. A linear, CNC-controlled x-y slide is used to define indentation and “steppover” (line spacing e.g. in meanders) distance on the specimen to be treated. These parameters, defining hammer head movement and path, allow for the introduction of RS states with variable maximum amount and degree of anisotropy. A soft bearing on top is used to determine contact properties and allow for load control. By this means, the “load fraction” [3] can be adjusted between non-contact and full contact.

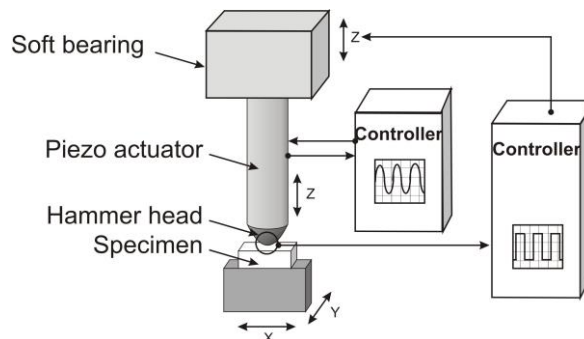


Fig. 1: Piezo peening (PP) process, schematic [2]

Deep cryogenic (cryo) treatments have been used for decades to reduce the content of retained austenite (RA) in martensitic tool steels by cooling work pieces down to $-196\text{ }^{\circ}\text{C}$ [5]. Combined with mechanical surface treatments, advantage can be taken of a range of beneficial effects. For instance, further RA gradients can be established by local mechanical deformation [6 – 9], whereby tailored surface characteristics such as hardness and RS profiles are achievable. Thus, beneficial combinations of “global” and “local” RA reduction can be obtained. Surface integrity resulting from such combined treatments has been investigated after deep rolling of AISI 304 metastable austenite [8, 9]. Increased near-surface hardness and thus enhanced wear resistance was found after cryo deep rolling [8]. Moreover, a relationship concerning thermal and mechanical energy proportions of transformation was established and applied to cryo deep rolling of AISI D3 tool steel [9].

Cryo-assisted plastic deformation is furthermore known to suppress the detrimental effect of heat on generation of compressive RS and to facilitate the formation of wear-inhibiting nanocrystalline surface layers [7, 10]. Depending on the material, further changes in relevant deformation mechanisms, such as twinning [11] and thermal activation [12] are expected. Regardless of the

applied material, the effects of such combined thermo-mechanical surface treatments are particularly worth investigating in the context of PP because a wide range of work-hardening and RS profiles can be generated using this process. The underlying medium to high [1] strain rates ($\sim 100/s$) during PP are expected to strongly interact with those temperatures with respect to the resulting flow stresses. This is due to the individual slip kinetics of bcc and fcc materials [12], where lower temperatures lead to higher yield stresses and stronger work-hardening, respectively. Using hardened, RA containing steels, both RS profile and anisotropy (due to volumetric expansion of mechanically induced martensite) can possibly be affected by applying cryo PP.

In this study, the effect of conventional and cryo PP on surface layers of RA containing hardened bearing steel AISI 52100 is investigated. Tailored RA and RS profiles, achieved by such modified treatments, are possibly beneficial for the mechanical behavior, such as wear resistance [8] and fatigue strength [7]. The latter is strongly affected by surface roughness, hardness and work-hardening state as well as RS profiles and stability. While crack initiation life is mainly governed by the resistance against dislocation movement, the amount of crack closure, which is enhanced by compressive RS generated due to transformation of RA at the crack tip, affects the driving force for crack propagation [13]. If existent, the most pronounced effect is expected to apply in the HCF range in strain-controlled tests. So, smooth surfaces of high hardness without near-surface martensite - austenite phase boundaries together with stable compressive RS can possibly enhance fatigue behavior of a material by using the combinatory effect of graded RA contents.

Objectives

This paper focuses on surface states after PP on hardened AISI 52100 with a RA content of approximately 13%. The scope of this study is to demonstrate the ability of PP to generate tailored RA profiles by adding the peening temperature to the common set of parameters. The effect of different PP treatments on near-surface RA, hardness and RS profiles as well as roughness is investigated. Furthermore, using flat as well as cylindrical specimens, respectively, the effect of those treatments on alternating and rotating bending fatigue behavior is studied.

Methodology

PP treatments were carried out at the test bench developed at KIT [2]. The necessary modifications for cryo treatment of flat and cylindrical specimens are shown in Fig. 2. Prior to PP, specimens were cooled down to $-180\text{ }^{\circ}\text{C}$ for 120 minutes using liquid N_2 flowing through brass block specimen holders. Cylindrical specimens were rotated by a DC electric motor within the cooling block during PP treatment. By this means, meanders and helixes were created on flat and cylindrical specimens, respectively. The cooling process was controlled by means of a two-point temperature controller. All remaining process parameters were kept constant: Load fraction: 0.5; frequency: 500 Hz; stroke: $36\text{ }\mu\text{m}$; stepover distance: $250\text{ }\mu\text{m}$; spherical WC-Co hammer head with 5 mm diameter.



Fig. 2: Cryo PP devices for flat specimens (left) and cylindrical specimens (right)

The bearing steel AISI 52100 (100Cr6) with a micro hardness of approximately 810 HV1 was used for the investigations. Its chemical composition is shown in Tab. 1. The material was austenitized at 860 °C for 20 minutes, oil-quenched and afterwards tempered at 180 °C for 60 minutes for moderate RA stabilization. Then, it was furnace-cooled to room temperature. By this means, a RA content of approximately 13% was obtained. Flat and cylindrical specimens (drawing in Fig. 3) were used for the investigations. The former were applied for characterization of surface layer states and for alternating bending tests. After heat treatment, they were mechanically ground to a surface roughness of $R_a = 0.33 \mu\text{m}$, which was necessary for proper PP process conditions. Since cracks often emerged at edges, cylindrical specimens were used in rotating bending tests to better assess the fatigue behavior. They were rough-machined, heat-treated and subsequently hard-finished.

Table 1: Chemical composition of AISI 52100 (wt.-%)

Fe	C	Cr	Mn	Si	Al	Ni
Base	1.08	1.45	0.36	0.23	0.03	0.03

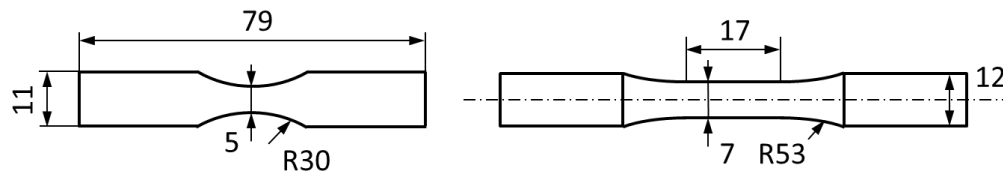


Fig. 3: Geometry of flat specimens (left) and cylindrical specimens (right)

Near-surface RS and RA measurements were carried out in the center of the peened area on flat specimens, using x-ray diffraction. RS were evaluated using V-filtered Cr- K_{α} radiation on the $\{211\}$ - α -ferrite diffraction line at $2\theta = 156.4^{\circ}$. X-ray stress analysis was carried out according to the $\sin^2(\psi)$ method [14], using $E\{211\} = 220 \text{ GPa}$ and $\nu\{211\} = 0.28$ as Young's modulus and Poisson's ratio, respectively. RA contents were evaluated using Zr-filtered Mo- K_{α} radiation. Diffraction angles 2θ between 20° and 60° were used, taking into account the $\{200\}$ -, $\{211\}$ -, $\{321\}$ -interference lines of the martensite phase and the $\{200\}$ -, $\{220\}$ -, $\{311\}$ -interference lines of the RA phase. For data evaluation the integrated peak intensities for each diffraction peak were determined using a PVII fit function. Then the phase fraction of RA was calculated according to the procedure described in [15]. RS and RA depth profiles were determined by incremental electrolytic layer removal.

Surface states were further characterized by means of micro hardness (HV0.1) and topography measurements. S/N curves were derived for untreated, conventionally and cryo-peened specimens by means of alternating and rotating bending fatigue tests. Three deflection-controlled Schenck alternating bending machines and a SincoTec rotating bending test bench with a LabView-based momentum controller were used, respectively. Based on preliminary experiments on untreated specimens, two or more load amplitudes in the HCF and upper LCF range were selected.

Results and analysis

RA fractions and micro hardness distributions in untreated and differently treated specimens are shown in Fig. 4. Due to RA stabilization, merely applying cryogenic temperatures has only a weak effect on the overall RA fraction, which is around 13% in untreated and around 12% in cryogenically cooled specimens. However, the near-surface (depth $< 250 \mu\text{m}$) RA content could be reduced by applying PP, and even more pronounced, by cryo PP. The latter reduces the RA fraction to values $< 5\%$ in an affected near-surface area which is found to be larger than after conventional PP. Furthermore, there seems to be a RA minimum at $100 \mu\text{m}$ depth after cryo PP, which does not exist after conventional PP. This effect is also visible in Fig. 4 (right), where micro hardness

distributions after the aforementioned treatments are shown. Besides the visible micro hardness maximum occurring after cryo PP, the bulk hardness is slightly increased.

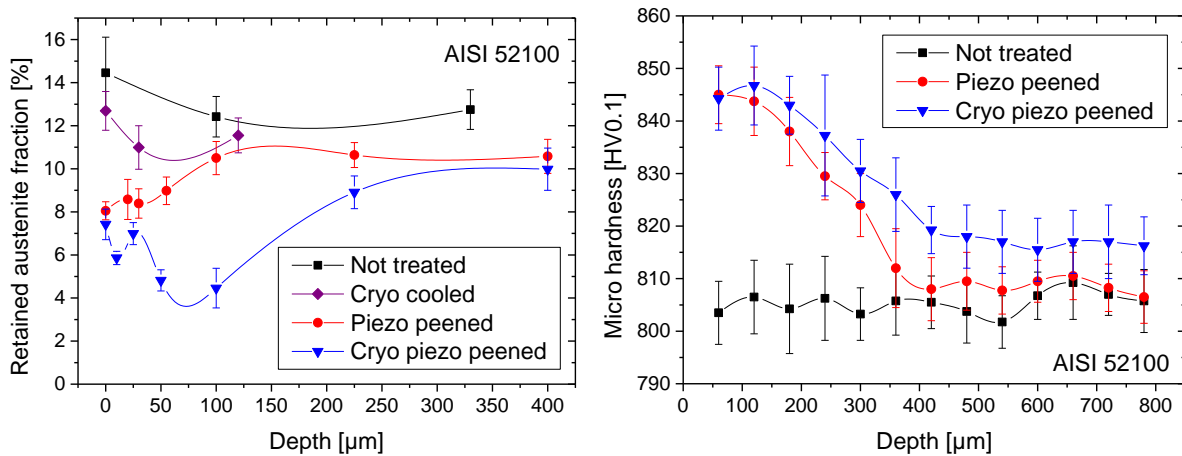


Fig. 4: Retained austenite fraction (left) and micro hardness distribution (right)

Fig. 5 shows transverse (referred to feed direction) residual stress profiles together with some single longitudinal measurements (left) and FWHM distributions (right) after the aforementioned treatments. A pronounced residual stress minimum was found for both treatments. However, penetration depth after cryo PP seems to be slightly increased. The degree of surface RS anisotropy was found to be very low for the chosen parameter set in both cases. FWHM values, measured only in the martensite phase, were found to decrease due to work-softening.

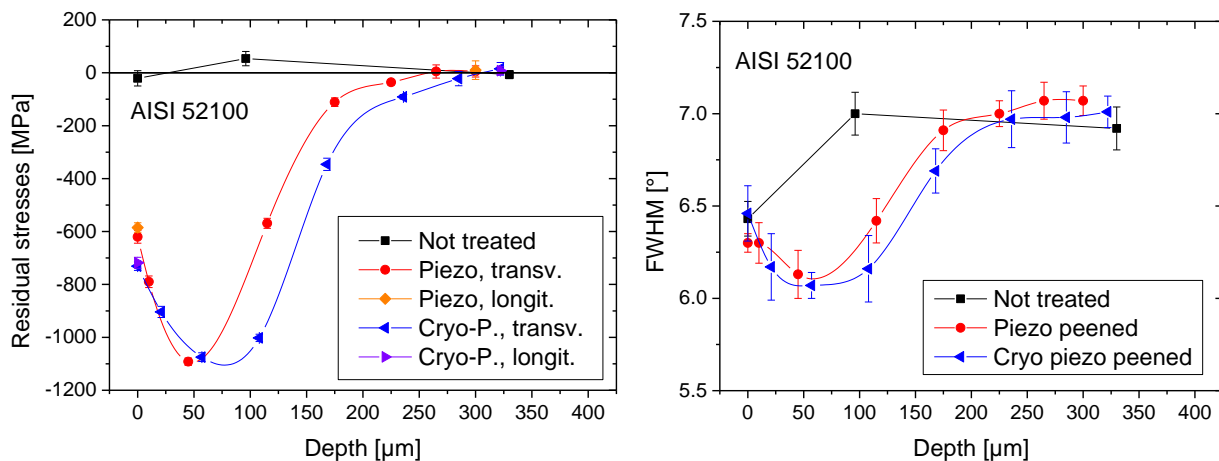


Fig. 5: Residual stress profiles (left) and FWHM distributions (right)

Furthermore, the application of cryogenic conditions to PP has some effect of the resulting surface roughness. In the untreated state, the surface roughness was $R_a = 0.33$. This value was lowered to $0.18 \mu\text{m}$ and $0.17 \mu\text{m}$ after conventional and cryo PP, respectively. Since low roughness values combined with near-surface hardness gradients can possibly enhance fatigue behavior, alternating bending fatigue tests were carried out. The corresponding S/N curves are shown in Fig. 6 (left). The fictitious stress amplitude σ_a^* in the extreme fiber is shown as a function of the number of cycles to failure N_f . Obviously, the S/N curve does not show any tendency and is rather characterized by pronounced scatter of fatigue lives, particularly on untreated specimens. On many specimens fatigue cracks emanated at edges, which might have been due to unreachability during PP. However,

since results were still promising, rotating bending fatigue tests were carried out using specimens shown in Fig. 3. The results of these tests are shown in Fig. 6 (right).

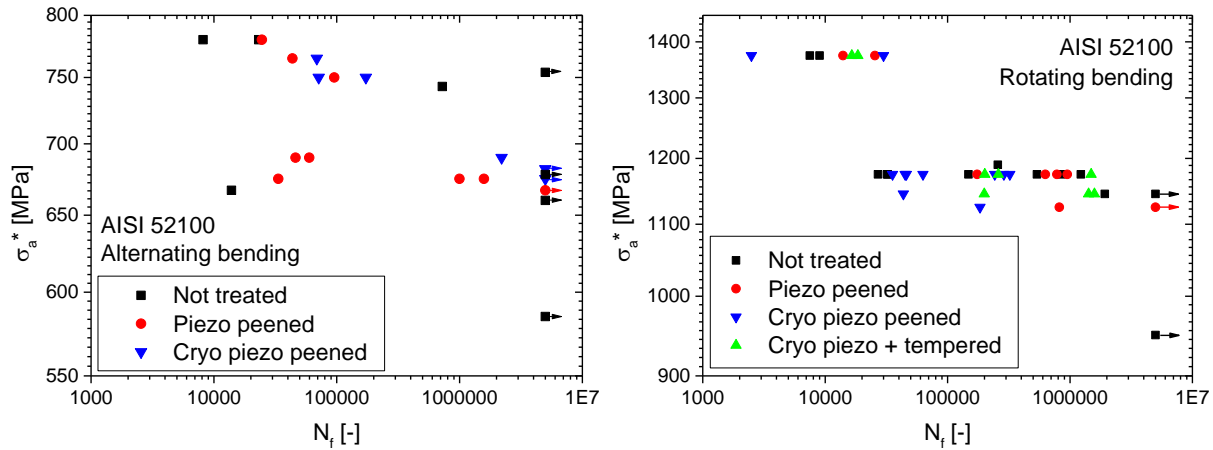


Fig. 6: S/N curves of alternating (left) and rotating (right) bending fatigue tests

Rotating bending fatigue lives can be enhanced by conventional PP in the LCF range ($\sigma_a^* = 1375$ MPa), while the effect is not pronounced in the HCF range. The initially high scatter in fatigue lives is apparently lowered by PP. However, no beneficial effect could be achieved by merely applying cryogenic cooling to PP. Fatigue lives were not only shortened, but the initial scatter remained unchanged. This effect is possibly due to the higher penetration depths of initially brittle martensite compared to conventional PP. To overcome this detrimental effect, some specimens were tempered another 60 min at 180 °C after cryo PP treatment. By this means, fatigue lives were prolonged again and scatter apparently reduced in the HCF range. Due to the small number of specimens used, the assumption of the latter effect is rather speculative. However, a similar effect was detected by [16], who found a reduction of scatter in fatigue tests after tempering subsequent to deep cryogenic treatment of case hardened UNI 7846 (18NiCrMo5). Thus, with the chosen parameters of this investigation, fatigue lives could not be increased markedly, but possibly enhanced in terms of scatter. Yet, the underlying reasons are subject to discussion. [7] found a strong influence of stability of surface characteristics on fatigue performance. Residual stress stability can be increased by tempering-induced static strain ageing [17] and thus contributes to fatigue life enhancement. However, since crack initiation to propagation ratios of fatigue lives have not been investigated, the underlying mechanisms of fatigue are still subject to characterization.

Besides the visible micro hardness maximum occurring after cryo PP, it is obvious from the slightly higher bulk hardness that a small fraction of RA was transformed into martensite due to cryo cooling. Obviously, thermal and mechanical energy partitions contribute to the formation of retained austenite gradients, as previously described by [9]. Furthermore, two different mechanical mechanisms, namely stress-induced and strain-induced transformation, might play a role in this investigation [18]. Stress-induced RA transformation is known to occur in low temperature ranges at unstable RA. Strain-induced RA transformation is known to occur in elevated temperature ranges and when the RA is rather stabilized. So, the former mechanism might explain the decreased RA content after PP even in high penetration depths, while the latter mechanism is responsible for further, gradients in the region $< 250 \mu\text{m}$. Yet, this finding cannot explain the sub-surface minimum of the RA content. Similar effects regarding residual stress profiles have been found after cryo PP on AISI 4140 (no RA) [19] as well as after deep rolling of AISI 304 austenitic stainless steel [7]. Applying cryo cooling to PP and deep rolling obviously shifts deformation beneath the surface, regardless of material and RA fraction. As aforementioned, bcc materials show higher yield strengths at lower temperatures and increased strain rates, while the hardening curves are hardly

affected. In contrast, fcc materials show a strong temperature and strain rate dependence of work-hardening [12]. Thus, the effect can possibly be explained in terms of a temperature-induced increasing contribution of Hertzian pressure [17] to near-surface plastic deformation. However, this effect is difficult to isolate, since the interaction between stress state, strain rate, temperature, adiabatic heating and flow stresses is complex. Thus, more attention should be devoted to such thermo-mechanical effects in future studies.

Conclusion

A combined thermo-mechanical surface treatment, consisting of the machine hammer peening treatment "piezo peening" and deep cryogenic cooling, was proposed. It was motivated by the study of deformation mechanisms and resulting surface layer states on the one hand, and possible effects upon service life on the other hand. So, tailored retained austenite contents could be achieved. Service life was evaluated by bending fatigue tests. Piezo peening and cryo piezo peening did not enhance fatigue lives significantly, but combined with further tempering, a reduction of fatigue scatter was assumed. Further investigations must focus on soaking time and temperature, which are important process parameters in cryogenic treatments. Future studies could also be extended to a material system with a higher RA content, such that any occurring effect will be more pronounced.

References

- [1] Schulze, V., et al. "Surface modification by machine hammer peening and burnishing." *CIRP Annals-Manufacturing Technology* 65.2 (2016): 809-832.
- [2] Lienert, F., et al. "Residual stress depth distribution after piezo peening of quenched and tempered AISI 4140." *Materials Science Forum*. Vol. 768. Trans Tech Publications, 2014.
- [3] Lienert, F. et al. "Changes in surface layer after Piezo Peening of quenched and tempered AISI 4140", in *Proc. ICSP12 (2014)*, pp. 511-516.
- [4] Lienert, F., et al. "Influence of Piezo Peening on the Fatigue Strength of quenched and tempered AISI 4140", in *Proc. ICSP12 (2014)*, pp. 517-522.
- [5] Molinari, A., et al. "Effect of deep cryogenic treatment on the mechanical properties of tool steels." *Journal of materials processing technology* 118.1 (2001): 350-355.
- [6] Altenberger, I. "Deep rolling—the past, the present and the future.", in *Proc. ICSP9 (2005)*.
- [7] Nikitin, I., and Scholtes, B. "Deep rolling of austenitic steel AISI 304 at different temperatures—near surface microstructures and fatigue." *HTM Journal of Heat Treatment and Materials* 67.3 (2012): 188-194.
- [8] Meyer, D., et al. "Surface hardening by cryogenic deep rolling." *Procedia Engineering* 19 (2011): 258-263.
- [9] Meyer, D. "Cryogenic deep rolling—An energy based approach for enhanced cold surface hardening." *CIRP Annals-Manufacturing Technology* 61.1 (2012): 543-546.
- [10] Kaynak, Y., et al. "Cryogenic machining-induced surface integrity: a review and comparison with dry, MQL, and flood-cooled machining." *Machining Science and Technology* 18.2 (2014): 149-198.
- [11] Sarma, V., et al. "Role of stacking fault energy in strengthening due to cryo-deformation of FCC metals." *Materials Science and Engineering: A* 527.29 (2010): 7624-7630.
- [12] Mecking, H., and Kocks, U.F. "Kinetics of flow and strain-hardening." *Acta Metallurgica* 29.11 (1981): 1865-1875.
- [13] Suresh, Subra. *Fatigue of materials*. Cambridge university press, 1998.
- [14] Macherauch, Eckard, and Paul Müller. "Das $\sin^2\psi$ -Verfahren der röntgenographischen Spannungsmessung." *Z. angew. Phys* 13.7 (1961): 305-312.
- [15] Faninger, G., and U. Hartmann. "Physikalische Grundlagen der quantitativen röntgenographischen Phasenanalyse (RPA)." *HTM* 27 (1972): 233-244.
- [16] Baldissera, Paolo. "Fatigue scatter reduction through deep cryogenic treatment on the 18NiCrMo5 carburized steel." *Materials & Design* 30.9 (2009): 3636-3642.
- [17] Schulze, Volker. *Modern mechanical surface treatment: states, stability, effects*. John Wiley & Sons, 2006.
- [18] Tamura, I. "Deformation-induced martensitic transformation and transformation-induced plasticity in steels." *Metal Science* 16.5 (1982): 245-253.
- [19] Klumpp, A., et al. "Residual Stress States After Piezo Peening Treatment at Cryogenic and Elevated Temperatures Predicted by FEM Using Suitable Material Models." *Proc. ICRS10 (2016)*.